Solar Energy Materials & Solar Cells 120 (2014) 724–727

Contents lists available at ScienceDirect

Solar Energy Materials & Solar Cells

journal homepage: www.elsevier.com/locate/solmat

Organic solar cells comprising multiple-device stacked structures exhibiting complementary absorption behavior

Wei-Ting Lin [a], Yen-Tseng Lin [b], Chu-Hsien Chou [a], Fang-Chung Chen [a,*], Chain-Shu Hsu [c]

[a] Department of Photonics, National Chiao Tung University, Hsinchu 30010, Taiwan
[b] Institute of Lighting and Energy Photonics, National Chiao Tung University, Tainan 71150, Taiwan
[c] Department of Applied Chemistry, National Chiao Tung University, Hsinchu 30010, Taiwan

ARTICLE INFO

Available online 28 August 2013

Keywords:
Organic
Photovoltaic
Multi-junction
Absorption

ABSTRACT

We developed organic solar cells based on multiple-device stacked structures featuring complementary absorption behavior. The first, semitransparent (ST) subcell featured an inverted structure; its anode comprised a MoO_3/Ag bilayer. This structure provided a transmittance of greater than 35% in the visible region. The second subcell, featuring a low-band-gap small molecule in its photoactive layer, was stacked onto the ST device; the two subcells could be connected either in series or in parallel. Because the two subcells exhibited complementary absorption behavior, their stacked structure connected in parallel displayed a power conversion efficiency of 4.37%, greater than those of the isolated subcells.

1. Introduction

Organic photovoltaic devices (OPVs) are promising candidates for use in next-generation solar cells because of their attractive properties of inexpensive fabrication, light weight, and mechanical flexibility [1–6]. The presence of bulk heterojunctions between the electron donors and acceptors in photoactive thin films can greatly improve device efficiency [1–6]. To date, the power conversion efficiency (PCE) of OPVs has reached approximately 10% in single-junction devices [1]. Increasing photon absorption is one of the key issues that must be overcome if we are to further improve PCEs. The low mobility of organic materials, however, restricts the use of thicker photoactive layers for the harvesting of greater number of photons. Moreover, the narrow absorption ranges of single materials limit the range of the solar spectrum available for absorption. One plausible method toward solving these problems is to produce tandem cells [7–11]. Nevertheless, because multi-junction devices have relatively complicated structures, the need for sophisticated fabrication procedures generally decreases the device fabrication yield.

In 2006, Shrotriya et al. proposed an alternative approach for constructing multi-junction devices: they superimposed one semi-transparent (ST) cell onto another conventional one [12]. After connecting the two subcells, either in series or in parallel, the PCE could be doubled relative to the efficiency of the corresponding single-junction device. Nevertheless, most reported stacked cells of this type have adopted the same photoactive materials in the two subcells [12–14]; as a result, multiple-device stacked structures exhibiting complementary absorptions are rare [15]. In this present study, we used two different organic materials, with complementary absorption spectra, as the photoactive layers in the two subcells. The first, ST subcell adopted an inverted structure; its ST anode comprised a MoO_3/Ag bilayer. The second subcell featured a low-band-gap (LBG) small molecule (SM) in its photoactive layer; it was stacked onto the ST device such that the two subcells were connected either in series or in parallel. Because the absorption behavior of the two subcells was complementary, the stacked device exhibited improved PCE relative to that of the single-cell device.

2. Experimental

The conjugated polymer and fullerene derivative used in this study were regioregular poly(3-hexylthiophene) (P3HT) and 1-(3-methoxycarbonyl)propyl-1-phenyl[6,6]methanofullerene (PCBM), respectively. The LBG SM used in the back subcell was 2,5-di(2-ethylhexyl)-3,6-bis-(5″-*n*-hexyl-[2,2′,5′,2″]terthiophen-5-yl)-pyrrolo[3,4-*c*]pyrrole-1,4-dione (SMDPPEH) [16]. Fig. 1(a) displays the chemical structures of these materials as well as the device structure. Fig. 1(b) presents the absorption spectra of the P3HT:PCBM and SMDPPEH:PCBM thin films. The two blends cover the solar spectrum over the range from 350 to 800 nm in a complementary manner. To begin the fabrication of the ST device, a solution of Cs_2CO_3 in 2-ethoxyethanol was spin-coated onto an indium tin oxide (ITO)-coated substrate and then the substrate was baked at 140 °C for 20 min. Next, a solution of the P3HT/PCBM blend in 1,2-dicholorobenzene was coated onto the substrate.

* Corresponding author. Tel.: +886 3 5131484; fax: +886 3 5735601.
E-mail address: fcchen@mail.nctu.edu.tw (F.-C. Chen).

0927-0248/$ - see front matter © 2013 Elsevier B.V. All rights reserved.
http://dx.doi.org/10.1016/j.solmat.2013.07.043

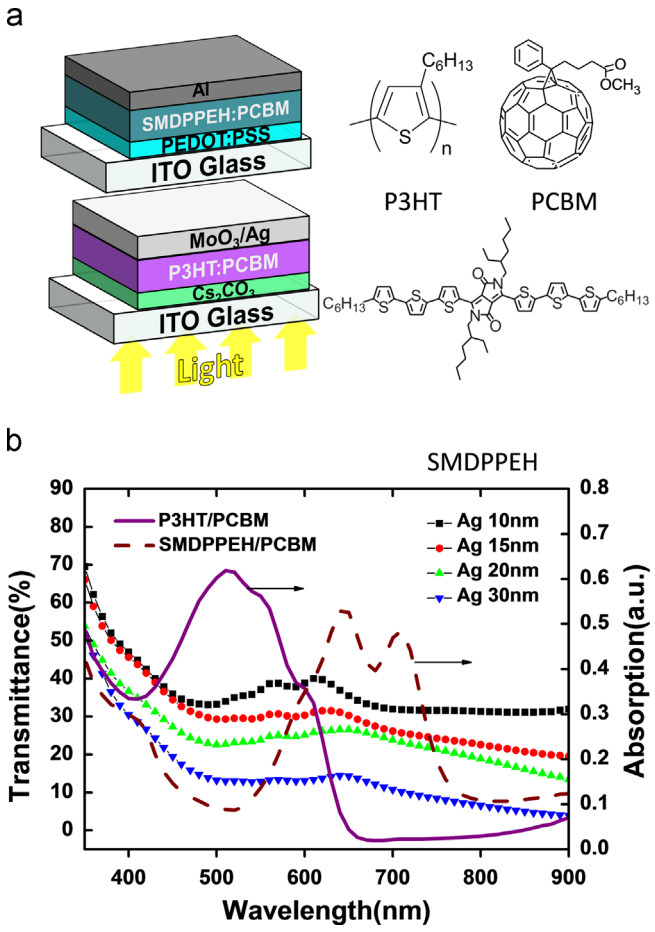

Fig. 1. (a) Chemical structures of P3HT, PCBM, and SMDPPEH. (b) Absorption spectra of films of P3HT:PCBM (1:1, w/w) and SMDPPEH:PCBM (1:1, w/w).

After solvent annealing [17,18], the sample was further thermally annealed at 110 °C for 15 min. Finally, MoO_3 (3.5 nm) and Ag (10–100 nm) were deposited to form the top electrodes; the Ag layer was chosen because of its long skin depth and high electrical conductivity [13]. Fabrication of the SM device began with spin-coating of poly(3,4-ethylenedioxythiophene):polystyrenesulfonate (PEDOT:PSS) onto an ITO-coated substrate and then baking the resulting film at 120 °C for 1 h. Next, a solution of the SMDPPEH:PCBM blend in chlorobenzene was coated on top of the PEDOT:PSS layer. Finally, Al (100 nm) was thermally evaporated to serve as the cathode. The photocurrent density–voltage (*J*–*V*) curves under illumination were recorded using a Keithley 2400 measurement system. The light source was a Thermal Oriel solar simulator, the illumination intensity of which was calibrated using a Si photodiode detector equipped with a KG-5 filter (Hamamatsu) [19].

3. Results and discussion

Fig. 2(a) displays the *J*–*V* curves of ST devices fabricated with various Ag thicknesses. Although the device fabricated with a 10-nm-thick Ag anode had the highest transmittance [Fig. 1(b)], it exhibited relatively poor performance, with a PCE of 2.36%. When we increased the thickness of the Ag layer to 15 nm, the transmittance in the visible region was greater than 35% [Fig. 1(b)]; this ST device exhibited an open-circuit voltage (V_{oc}) of 0.57 V, a short-circuit current (J_{sc}) of 8.53 mA cm^{-2}, and a fill factor (FF) of 0.61, leading to a PCE of 2.97%. In general, the device efficiency improved upon increasing the thickness of the Ag layer, suggesting

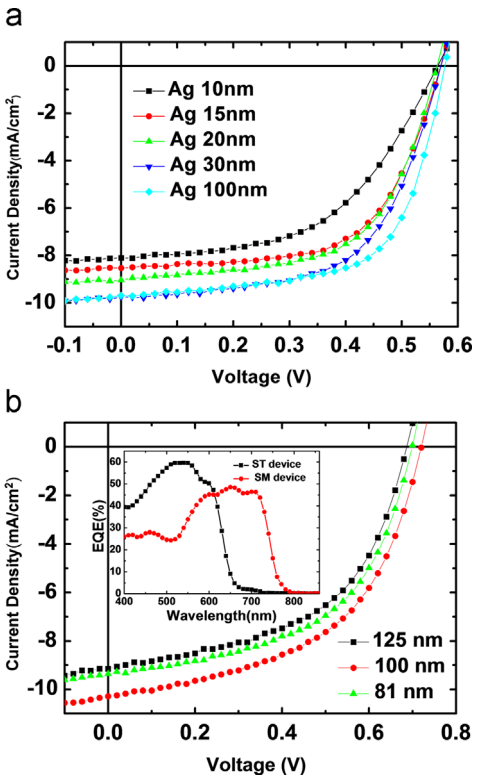

Fig. 2. (a) *J*–*V* characteristics of ST devices prepared with Ag layers of various thicknesses. (b) *J*–*V* curves of SM devices prepared with photoactive layers of various thicknesses. Inset: EQE spectra of the two subcells in the stacked structure. Structures of the ST and SM devices: ITO/PEDOT:PSS/P3HT:PCBM (220 nm)/MoO_3 (3.5 nm)/Ag and ITO/PEDOT:PSS/SMDPPEH:PCBM (100 nm)/Al, respectively.

Table 1
Photovoltaic parameters of OPVs featuring Ag anodes of various thicknesses.

Ag thickness (nm)	V_{oc} (V)	J_{sc} (mA cm^{-2})	**FF**	**PCE** (%)
10	0.56	8.10	0.52	2.36
15	0.57	8.53	0.61	2.97
20	0.57	9.03	0.60	3.03
30	0.57	9.74	0.59	3.29
100	0.57	9.70	0.65	3.57

that the sheet resistance of the Ag anode limited the device performance. Although the highest device efficiency (3.29%) was obtained when the thickness of the Ag layer was 30 nm, the overall transmittance in the visible wavelength range was only approximately 10% [Fig. 1(b)], making this device unsuitable for use in stacked structures. Table 1 summarizes the parameters of the devices featuring Ag anodes of various thicknesses.

Fig. 2(b) presents the *J*–*V* characteristics of the SM devices obtained under the illumination with simulated solar irradiation. For the optimized device, in which the thickness of the photoactive layer was 100 nm, the values of V_{oc}, J_{sc}, and FF were 0.72 V, 10.28 mA cm^{-2}, and 0.52, respectively, yielding a PCE of 3.83%. The inset to Fig. 2(b) displays the incident photon-to-electron conversion efficiencies (IPCEs) of both the ST and SM devices. The major wavelength response ranges of the ST and SM devices were 450–600 and 600–750 nm, respectively, confirming the complementary manner of photoabsorption of these two different devices.

We constructed multiple-device stacked structures by stacking the SM device onto the inverted ST device (Fig. 1); the back SM device absorbed solar irradiation that had passed through the ST device. We tested the performance of the two subcells connected either in parallel or in series. Fig. 3(a) displays the *J*–*V* curves of the